Geomagnetic field intensity variations in Western Europe over the past 1100 years

A. Genevey, Y. Gallet, E. Thébault, S. Jesset, M. Le Goff

Geochemistry Geophysics Geosystems G3

Article
Volume 14, Number 8
9 August 2013
doi: 10.1002/ggge.20165
ISSN: 1525-2027

Published by AGU and the Geochemical Society

Geomagnetic field intensity variations in Western Europe over the past 1100 years

A. Genevey
UPMC Univ. Paris 06, Laboratoire d'archéologie moléculaire et structurale, LAMS, 75005, Paris, France (agnes.genevey@upmc.fr)

CNRS, UMR 8220, LAMS, 75005, Paris, France

Y. Gallet and E. Thébault
Institut de Physique du Globe de Paris, Sorbonne Paris Cité, Université Paris Diderot, UMR CNRS 7154 , Paris, France

S. Jesset
Service archéologique de la ville d'Orléans, Orléans, France

M. Le Goff
Institut de Physique du Globe de Paris, Sorbonne Paris Cité, Université Paris Diderot, UMR CNRS 7154 , Paris, France

[1] Ten archeointensity results have been obtained from brick and ceramic fragments collected in France and precisely dated to between the tenth and eighteenth centuries. Intensity experiments were performed using the Triaxe protocol taking into account cooling rate and thermoremanent magnetization anisotropy effects. Together with our previous results from France and Belgium, we computed a geomagnetic field intensity variation curve for Western Europe covering the past 1100 years. This curve is characterized by a general decreasing trend at the millennial timescale punctuated by three short intensity peaks, during the twelfth century, around 1350–1400 AD and ~1600 AD. A similar evolution but with smoother variations due to data scatter is also observed in Western Europe and to a lesser extent in Eastern Europe when all available archeointensity data fulfilling quality criteria are used. Comparison of our archeointensity variation curve with the climatic record derived from fluctuations in length of the Swiss glaciers shows a good temporal concordance between all geomagnetic field intensity maxima detected in Western Europe over the past millennium and colder episodes. A comparison is further discussed between these intensity maxima and episodes of low rates of ^{14}C production. A common pattern of variations between both records is recognized between the middle of the tenth and of the beginning of eighteenth centuries. If significant, such coincidences suggest a dual geomagnetic and solar origin for the century-scale climate and radionuclide production variations during at least the past millennium.

Components: 8,855 words, 5 figures, 1 table.

Keywords: archeointensity; holocene; France; Europe; climate; 14C.

Index Terms: 1503 Archeomagnetism: Geomagnetism and Paleomagnetism; 1521 Paleointensity: Geomagnetism and Paleomagnetism; 1522 Paleomagnetic secular variation: Geomagnetism and Paleomagnetism; 9335 Europe: Geographic Location.

Received 21 February 2013; **Revised** 17 April 2013; **Accepted** 29 April 2013; **Published** 9 August 2013.

Genevey, A., Y. Gallet, E. Thébault, S. Jesset, and M. Le Goff (2013), Geomagnetic field intensity variations in Western Europe over the past 1100 years, *Geochem. Geophys. Geosyst.*, *14*, 2858–2872, doi:10.1002/ggge.20165.

1. Introduction

[2] Recovering details of Earth's magnetic field intensity variations over the past few millennia, beyond the recent and short (<200 years) "historical" period for which direct intensity measurements are available, remains a challenging task. At a regional scale, the dispersion often observed between intensity data of a similar age is puzzling [e.g., *Genevey et al*., 2008], which raises questions about our ability to retrieve from paleomagnetic analyses, short-term geomagnetic intensity variations. This scatter was previously discussed and interpreted as possibly reflecting an accuracy limit in the intensity data [*Gómez-Paccard et al*., 2006], whose errors could be severely underestimated as recently proposed by *Suttie et al*. [2011] from a statistical analysis of archeointensity results dated to the "historical" period. On the other hand, large and coherent intensity variations have been observed from archeointensity data obtained in Europe, Brazil, and the Middle East [*Gallet et al*., 2008; *Genevey et al*., 2009; *Schnepp et al*., 2009; *Hartmann et al*., 2011]. This seems to support the assertion that it is possible to detect and reliably recover rapid regional intensity variations as long as the data are well dated and experimentally well constrained.

[3] Assessing the robustness of the rapid intensity fluctuations has important implications for reliable determination of centennial to millennial-scale dipole moment changes as deduced from global archeomagnetic and paleomagnetic databases [e.g., *Genevey et al*., 2008; *Knudsen et al*., 2008; *Donadini et al*., 2009; *Korte and Constable*, 2011; *Korte et al*., 2011]. Moreover, rapid intensity variations may be of particular interest because their maxima have been suggested as a means to trace the occurrence of archeomagnetic jerks which would correspond to episodes of maximum geomagnetic field hemispheric asymmetry associated with production and gathering of flux patches at the core-mantle boundary [*Gallet et al*., 2009a]. Archeomagnetic jerks were proposed as new century-scale geomagnetic events characterized by sharp curvature changes in direction synchronous with intensity maxima [*Genevey and Gallet*, 2002; *Gallet et al*., 2003]. *Gallet et al*. [2005, 2006] noted also an intriguing temporal synchronism between archeomagnetic jerks and cooling periods in the Western European-Eastern North Atlantic region. If significant, this synchronism could indicate, at least regionally, some connection between geomagnetic secular variation and climate over multidecadal scales, possibly through geomagnetic modulation of the galactic cosmic ray flux interacting with the atmosphere [*Gallet et al*., 2005, 2009b; *Usoskin et al*., 2008, 2010; *Courtillot et al*., 2007; *Knudsen and Riisager*, 2009]. Such a hypothesis, however, still requires testing, including through the acquisition of new archeointensity results. We present here new French archeointensity results, which, together with previously published data, allow construction of a continuous Western European geomagnetic field intensity variation curve for the past 1100 years. In particular, the new data provide further evidence for a short geomagnetic intensity maximum around the middle of the twelfth century AD [*Gómez-Paccard et al*., 2012], in addition to two other maxima that were described by *Genevey et al*. [2009] during the second half of the fourteenth century and around 1600 AD.

2. Archeological Sample Collection

[4] The new archeointensity data were obtained from analysis of eleven groups of baked clay archeological artifacts dated to between the end of the ninth century and the end of the eighteenth century, which were produced in workshops from northern France (Table 1). This collection is composed of two groups of architectural brick fragments (sites AM03 and ORLF01) and nine groups of ceramic fragments found either in a production context, i.e., in connection with a ceramic workshop, or in occupation layers (Table 1). In the latter case, careful attention was given to only select locally produced potsherds. For both production and occupation archeological contexts, typo-morphology analysis of the ceramics was used to ensure the temporal homogeneity of the groups and to constrain their dating. This analysis relies on recognition of characteristic elements of the pottery (in particular the color of the clay paste, the decoration and/or size and shape of morphological attributes such as the lip, the base or the handles of the pottery) and their comparison with a typo-chronological reference of production established for a given region (e.g., *Jesset* [2003], for the region around Orléans where 6 of the 11 groups were collected). As an example, the light-colored clay paste and the presence of small grooves on the surface of fragments from group ORL03 allow definitive dating to the High Middle Ages.

Table 1. New Archeointensity Data From 11 Groups of Ceramic and Brick Fragments Dated to the Past 1100 Years[a]

Archeomagnetic label	Location	Lat. (°N)	Long. (°E)	Age (AD)	Type of material	Archeological information	Dating Constraints	N frag. (n spec.) retained	F mean σF (μT)	F mean in Paris (μT)
RIV01	Paris	48.90	2.30	870–925	Potsherd (PC)	Exc. in the square of the Saint-Jacques Tower—Frag. with granular clay paste	Chronogical evolution of the typo-morphology of the ceramic and coin and historical context [*Lagarde et al.*, 2011]	10 (20)	74.4 ± 2.0	74.4
RIV02	Paris	48.90	2.30	870–925	Potsherd (PC)	Exc. in the square of the Saint-Jacques Tower—Frag. with fine clay paste	Chronogical evolution of the typo-morphology of the ceramic and coin and historical context [*Lagarde et al.*, 2011]	12 (25)	74.5 ± 1.1	74.5
RIV01 + RIV02[b]	Paris	48.90	2.30	870–925	Potsherd (PC)	Exc. in the square of the Saint-Jacques Tower	Chronogical evolution of the typo-morphology of the ceramic and coin and historical context [*Lagarde et al.*, 2011]	22 (45)	74.4 ± 1.5	74.4
NE08	Nevers	46.98	3.17	975–1025	Potsherd (OC)	Exc. of Saint-Genest Street—Silo 361 (phase 6c)	Chronostratigraphic context and chronogical evolution of the typo-morphology of the ceramic [*Ravoire*, 2007]	4 (10)	57.3 ± 3.0	58.4
ORL04	Orléans	47.90	1.90	1050–1100	Potsherd (OC)	Exc. of the Ilot de la Charpenterie—F105—Zone 1	Chronostratigraphic context and historical context and archeological context and chronogical evolution of the typo-morphology of the ceramic	5 (17)	60.3 ± 3.2	60.9
CHEV01	Chevreuse	48.70	2.05	1100–1150	Potsherd (OC)	Exc. in the Dungeon of the Madeleine Castle—SU 82012	Chronostratigraphic context and chronogical evolution of the typo-morphology of the ceramic [*Barat et al.*, 2010; Ravoire pers. comm.]	3 (8)	62.8 ± 1.6	62.9
ORL03	Orléans	47.90	1.90	1100–1175	Potsherd (PC)	Exc. of Jeanne d'Arc Street—Zone 1—SU 10062	Chronological evolution of the typo-morphology of the ceramic	8 (24)	65.7 ± 3.0	66.3
AM03	Abbey of Morimond	48.07	5.67	1160–1190	Brick	Foundations of a building located in an area intended for guests of the Abbey	Historical constraints and stylistic elements confirmed by radiocarbon dating [*Rouzeau*, 2009, 2010]	3 (11)	56.4 ± 1.1	56.9
FAL01	Fay-aux-Loges	47.93	2.14	1425–1475	Potsherd (PC)	Exc. of "La Loge Cogne" site	Chronogical evolution of the typo-morphology of the ceramic [*Jesset*, 2011]	4 (10)	54.0 ± 0.5	54.5
ORLF01	Orléans	47.90	1.90	1517–1518	Brick	Bricks from the façade of a half-timbered house located at 7 Bourgogne Street	Dendrochronology measurements performed on timbers [*C. Alix*, personal communication]	4 (12)	50.4 ± 0.8	50.9
ORL06	Orléans	47.90	1.90	1630	Potsherd (OC)	Exc. of Faubourg-Madeleine street—Frag. of ceramic used as pigeonholes—SU 9027	Archives [*Blanchard*, 2010]	9 (18)	54.1 ± 1.4	54.6
ORL01	Orléans	47.90	1.90	1797–1798	Potsherd (PC)	Exc. of Halmagrand Place, Manufacture of the Baubreuil widow	Archives and chronological evolution of the typo-morphology of the ceramic [*Jesset*, 2010]	8 (16)	44.4 ± 1.5	44.8

[a]PC (or OC) indicates potsherds found in a production context (or occupation context). Exc. stands for excavations, SU for stratigraphic unit, frag. for fragment and spec. for specimen. N frag. (or n spec.), number of different fragments (or specimens) retained per group for computing a mean intensity value; $F_{mean} \pm \sigma F$, mean intensity at group level and standard deviation in μT; $F_{mean\ in\ Paris}$, mean intensity in μT after reduction to the latitude of Paris (48.9°N) using the hypothesis of an axial dipole field.

[b]Master mean intensity value was computed from the intensity results obtained for fragments of RIV01 and RIV02 groups, both dated to the end of period of activity of the same workshop.

Morphological attributes of the two main types of pots from this ensemble further constrain the dating. The first type is a pot with ribbon-shaped lips whose profile is typical of the twelfth century. The second type is a pitcher with tubular spout and diametrically opposed handles, which is known to have existed only between the eleventh century and the second part of the twelfth century. The lip of this pitcher is even more age diagnostic with its evolution toward a thicker and shorter lip with a slanted profile, which has been recognized to occur during the mid twelfth century. Together, these elements allow constraining of the dating of the ORL03 group to between the beginning and third quarter of the twelfth century.

[5] Dates for the analyzed groups were further constrained by additional archeological and/or historical elements (Table 1 and Text S1, supporting information). This is, for instance, the case for the pigeon loft from ORL06, whose construction mentioned in state archives is precisely dated to 1630 AD and which was rediscovered during archeological excavations. The ceramic fragments collected from this edifice all have the same shape and present external traces of mortar: they were clearly identified as pigeonholes produced for this building.

[6] For one group (ORLF01), we note that the age relies solely on dendrochronological dating. Bricks from this group were discovered and collected during a restoration of a façade of a half-timbered house from the historical center of the city of Orléans. Bricks in the façade were used to fill the space between the wooden timbers and dendrochronology measurements were performed directly on the timbers.

[7] Between 7 and 40 fragments were collected per site depending on sampling possibilities (Table S1, supporting information). The AM03 group is, for example, from the foundations of a building located in an area intended for guests of the Morimond Abbey and the fragments were drilled in the seven bricks found in the base of a pillar of this building. Excavations at the foot of the Saint-Jacques Tower in Paris allowed discovery of numerous Carolingian ceramics, mainly waste from kilns. A larger sampling was therefore possible and two groups of fragments (RIV01 and RIV02) with different clay pastes were collected to explore the production variety of this important Parisian ceramic workshop dated to the ninth to tenth century transition.

3. Acquisition of New Archeointensity Data

[8] Intensity experiments were exclusively carried out using a protocol hereafter referred to as the Triaxe protocol. It derives from the *Thellier and Thellier* [1959] method and was designed for the Triaxe vibrating sample magnetometer developed at the Institut de Physique du Globe de Paris [*Le Goff and Gallet*, 2004]. This protocol is fully described by *Le Goff and Gallet* [2004] and its reliability was successfully tested against intensity results obtained from more classical protocols derived from the *Thellier and Thellier* [1959] method using a wide collection of archeological artifacts with different origins, types, conditions of production and with different magnetic properties [*Gallet and Le Goff*, 2006; *Genevey et al.*, 2009; *Hartmann et al.*, 2011]. The originality of the Triaxe protocol lies in the fact that magnetization measurements of a specimen under analysis (<1 cm^3 in volume) are performed automatically and continuously at high temperatures. It is also worth underlining that this procedure avoids any thermoremanent magnetization (TRM) anisotropy effects and that intensity values derived using the so-called *R*' ratios have been experimentally shown to be independent of the cooling rate effect [*Le Goff and Gallet*, 2004]. Furthermore, any bias due to the possible presence of multidomain grains should be limited because the original natural remanent magnetization (NRM) and laboratory TRM are acquired and demagnetized under the same conditions.

[9] Intensity experiments were performed on two to four specimens per archeological fragment among those having a magnetization strong enough to be reliably measured using the Triaxe magnetometer. We note that the sensitivity of the Triaxe was critical for this study, in particular for four sites (NE08, ORL04, CHEV01, and ORLF01, Table S1, supporting information) from which most of the fragments were weakly magnetized.

[10] The overall suitability of the fragments for archeointensity determinations, including the thermal stability of the magnetic mineralogy, was evaluated through the same quality criteria as

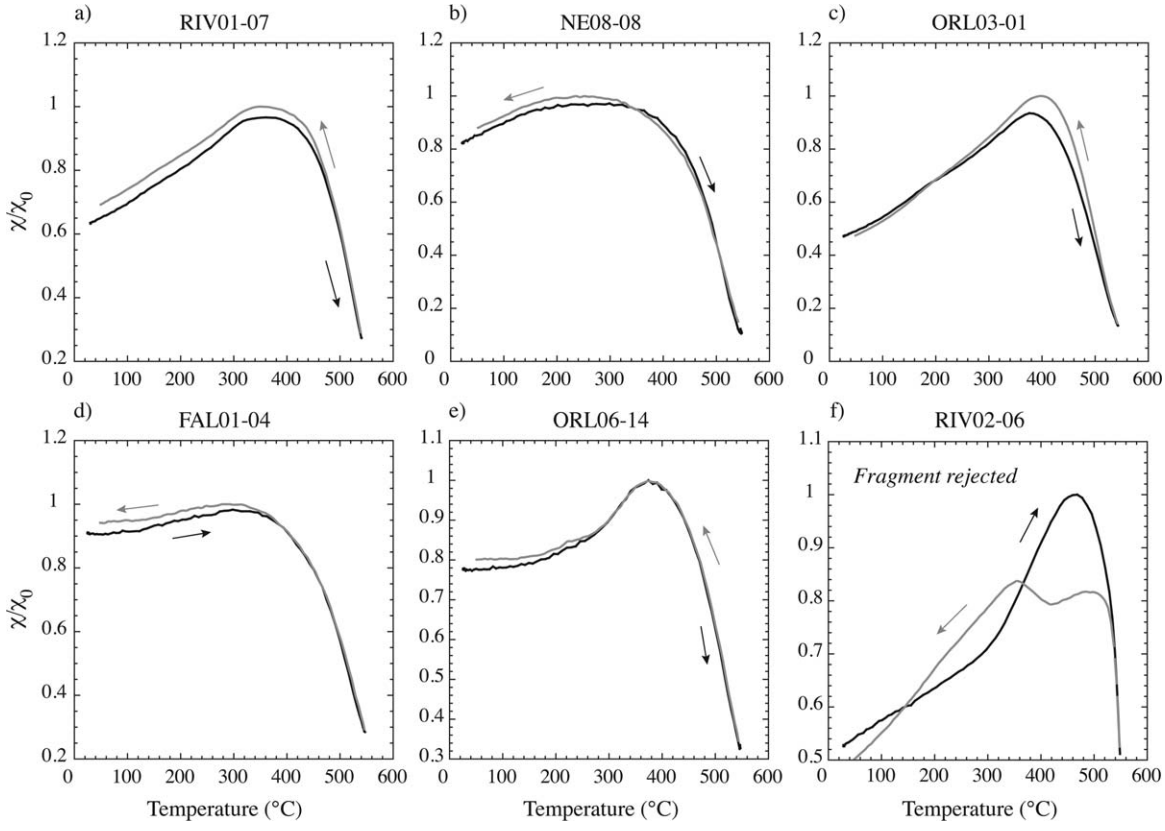

Figure 1. Normalized bulk low-field magnetic susceptibility versus temperature curves for different studied archeological fragments. (a–e) Examples of favorable behavior for archeointensity determinations. (f) Example of a rejected fragment because of high-temperature magnetic alteration.

those used by *Genevey et al*. [2009] and *Hartmann et al*. [2011] (Table S2, supporting information). These criteria aim to test the directional behavior, the quality of the intensity determinations and the coherence between results at the fragment and site levels. Additionally, the thermal stability of the magnetic mineralogy of each analyzed fragment was investigated by measuring variations of the low-field magnetic susceptibility up to maximum 550°C and back to room temperature using an Agico KLY3 Kappabridge system with CS3 heating attachment (Figure 1). This temperature was chosen because intensity analyses on the Triaxe magnetometer are always performed on a temperature interval whose maximum never exceeds 550°C. Any visible difference between heating and cooling curves, as shown in Figure 1f, resulted in rejection of the corresponding fragments. Considering the number of fragments effectively analyzed using the Triaxe magnetometer, i.e., whose magnetization was strong enough for analysis, the success rate of archeointensity measurements was between 40% and 100% (Table S1, supporting information).

[11] Isothermal remanent magnetization (IRM) acquisition and hysteresis measurements were conducted to further explore the magnetic mineralogy of the retained fragments. These fragments have variable magnetic properties, with large variability even within a site. For a few fragments, the IRM is saturated at low-magnetic fields (<0.3 T) and the shape of the hysteresis loops is nonconstricted (Figures 2a and 2b). Together with the almost complete demagnetization of the NRM below 550°C, these characteristics suggest that Ti-poor titanomagnetite in a pseudosingle domain state, as indicated by the hysteresis parameters, is the main carrier of the magnetization in those samples. For the other fragments, IRM is not saturated at 0.9 T and the hysteresis loops are clearly wasp-waisted (Figures 2a and 2c) [e.g., *Roberts et al*., 1995]. The NRM, which is nearly completely demagnetized below 550°C, and thermal evolution of low-field susceptibilities, suggest a magnetization carried by titanomagnetite and other magnetic minerals with low-unblocking temperatures and high coercivities. The latter minerals have been previously observed in archeological artifacts, with

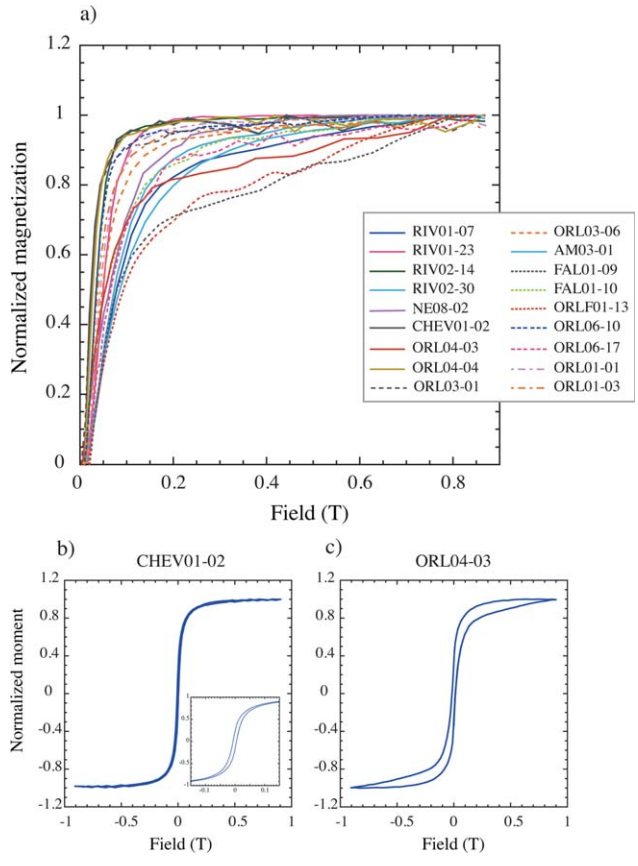

Figure 2. (a) Normalized IRM acquisition curves obtained for 18 representative pottery and brick fragments. Examples of a non-constricted hysteresis loop with (b) pseudosingle domain-like hysteresis parameters, and (c) a wasp-waisted hysteresis loop.

reliable intensity results obtained [e.g., *Chauvin et al*., 2000; *Genevey and Gallet*, 2002; *Hartmann et al*., 2011], but they have not yet been clearly identified [*McIntosh et al*., 2011].

[12] Intensity determinations that fulfill the quality criteria are reported in Figure 3 and Figure S1 in the supporting information (see also Table S1, supporting information), where each plot includes all data obtained from one site and each curve represents the intensity values obtained for one specimen using the *R*'(Ti) ratios within the temperature interval of analysis [*Le Goff and Gallet*, 2004]. The curves from each plot clearly underline the coherence of the new intensity results both at the fragment and site levels. This allows computation of site-mean intensity values with, in all cases, a standard deviation of less than 5.5% of the corresponding mean (Table 1). The site-mean results were obtained by first averaging the intensity values obtained from the same fragment and then the fragment values. For groups RIV01 and RIV02 associated with the same ceramic workshop, excellent agreement was observed between the two site-mean values (i.e., for both clay pastes) and a master site-mean intensity value was computed by averaging all data obtained from fragments (Table 1).

[13] In addition to the new archeological collection, we also reanalyzed using the Triaxe protocol the different fragments of group A02 previously studied by *Genevey and Gallet* [2002] using the *Thellier and Thellier* [1959] method as revised by *Coe* [1967]. The new Triaxe intensity values were found to be higher (of 18%) than those previously obtained, in good agreement with the intensity variations observed for the twelfth century (mean reduced at Paris 62.8 ± 2.1 μT; Table S1 and Figure S1, supporting informations). Although we strongly suspect that the cooling rate correction applied by *Genevey and Gallet* [2002] to the raw intensity value determined using the classical Thellier and Thellier method as revised by Coe, was overestimated leading to a too low-intensity value, we followed the same strategy adopted by

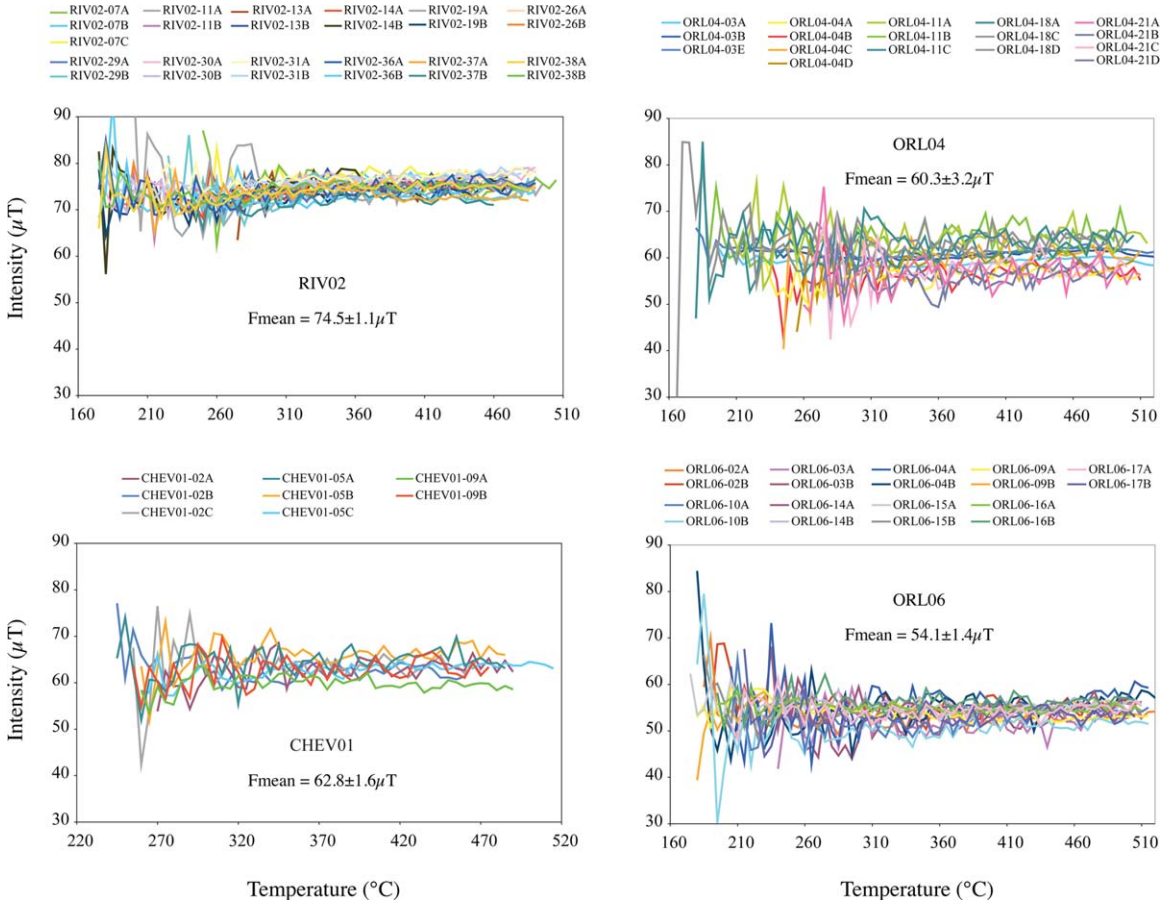

Figure 3. Intensity determinations that fulfill our selection criteria for four groups of archeological fragments. Individual curves represent the intensity values computed using the *R*'(Ti) ratios for one specimen over the temperature interval of analysis [*Le Goff and Gallet*, 2004] (see Figure S1, supporting information for intensity determinations from eight other groups of fragments).

Genevey et al. [2009] for a similar case and we have simply eliminated the problematical site. The cooling rate dependence of TRM acquisition is clearly a parameter that is difficult to estimate in archeomagnetism, not so much experimentally [*Chauvin et al*., 2000; *Genevey and Gallet*, 2002] but rather from an archeological viewpoint.

4. Discussion

[14] Because of the large scatter in archeointensity data in the current European database [e.g., *Genevey et al*., 2009], we first discuss our own data which forms a homogeneous data set both in terms of data acquisition and selection criteria, i.e., the data reported by *Genevey and Gallet* [2002], *Genevey et al*. [2009], and from this study, and then all of the available results from Western and Eastern Europe spanning the past millennium and fulfilling quality selection criteria.

[15] From our results, we are left with a collection of 46 French and two Belgian archeointensity values covering the past 1100 years (Figure 4a). Before 1200 AD, the new data appear to be of particular interest because they reveal a short intensity peak during the twelfth century. We also underline the good consistency between intensity variations from our previous results [*Genevey and Gallet*, 2002; *Genevey et al*., 2009] and the new data, which help to better constrain the successive intensity decreases during the tenth, fifteenth, and seventeenth centuries and also an intensity minimum around the end of the eighteenth century. We used an iteratively reweighted least-squares algorithm combined with a bootstrap approach in order to derive a master curve from this coherent data set (Figure 4a, see also Figure S3a, supporting information; *Thébault and Gallet* [2010]). The iteratively reweighted least-squares technique is designed to mitigate the effect of inconsistent intensity values while the bootstrap approach allows

also exploring the effect of dating and experimental errors on the master curve estimation. The algorithm computes a large ensemble of curves estimated from a statistically significant combination of intensity and dating errors that are then used to produce an archeointensity master curve in the form of a probability density distribution displayed with a gray scale in Figure 4 (see also Figure S3, supporting information). In the absence of experimental and dating biases, the arithmetic mean and the 95% envelope of the distributions should coincide almost exactly with the maximum likelihood and its 95% error bars derived from the more conventional least-squares approach. This is

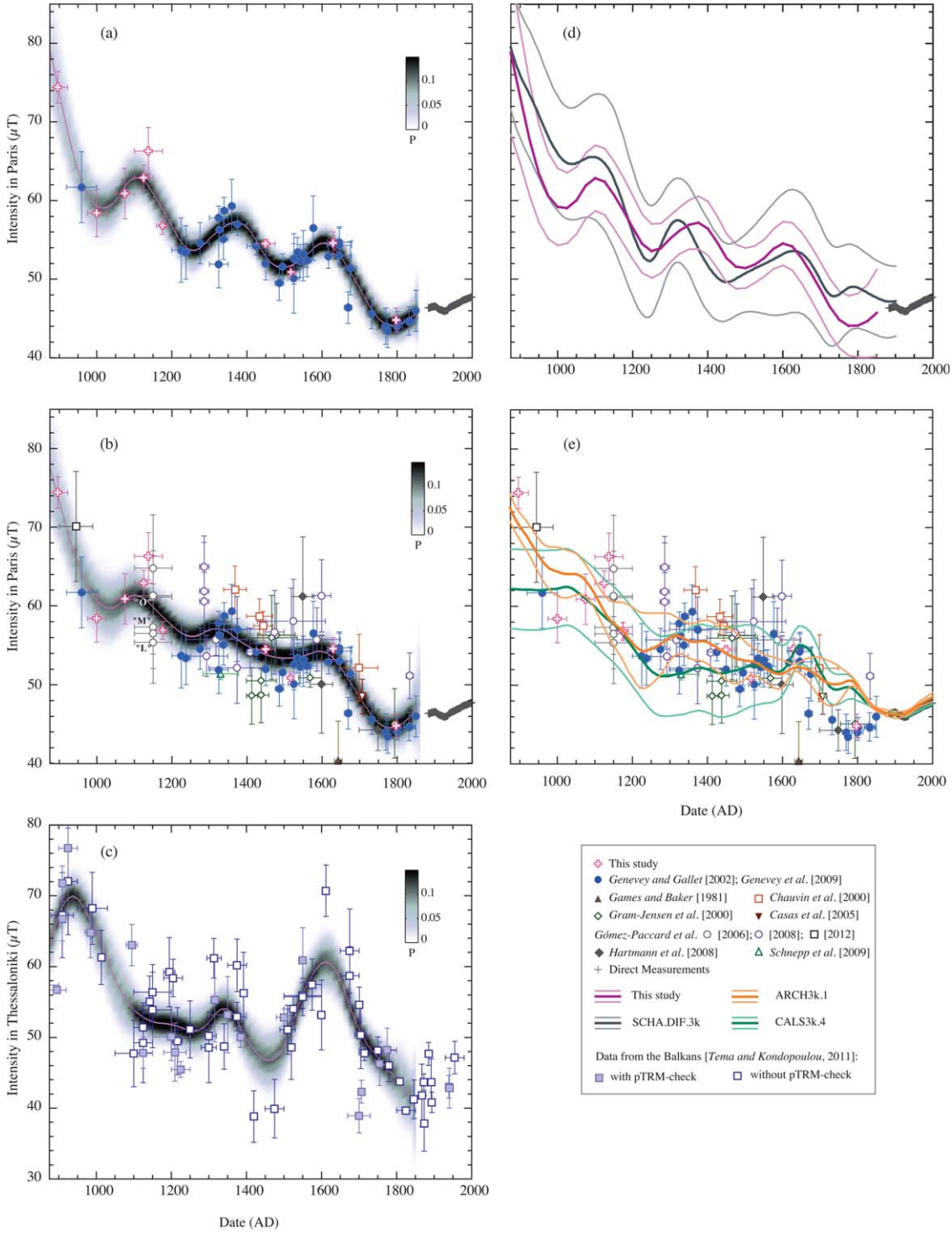

Figure 4. Geomagnetic field intensity variations in Europe over the past 1100 years (a) Variations in Western Europe deduced from our French and Belgian data [*Genevey and Gallet*, 2002; *Genevey et al*., 2009; this study]. Probability density distributions, computed using the algorithm of *Thébault and Gallet* [2010] with a *B*-spline knot spacing of 70 years, are represented by gray-shaded tones with their maxima reported in pink (same for Figures 4b and 4c). Direct measurements performed in France are from http://www.bcmt.fr/. All data were reduced to the latitude of Paris (48.9°N). (b) Variations in Western Europe deduced from our data and previous results that fulfill quality criteria for samples from France [*Chauvin et al*., 2000; *Gómez-Paccard et al*., 2012], Spain [*Gómez-Paccard et al*., 2006, 2008], Portugal [*Hartmann et al*., 2008], England [*Games and Baker*, 1981; *Casas et al*., 2005], Denmark and Norway [*Gram-Jensen et al*., 2000], and Germany [*Schnepp et al*., 2009]. A cooling rate correction with a 5% decrease was applied to data for which this effect was not taken into account (same for Figure 4c below). Note that "O", "M", and "L" refer to a stratigraphic succession of three Spanish kilns (see text) [*Gómez-Paccard et al*., 2006]. The NRMS is 1.5, which indicates that the master curve could not fit all data within their published *a priori* uncertainties. (c) Variations in Eastern Europe deduced from Greek and Bulgarian data that fulfill quality criteria [*Tema and Kondopoulou*, 2011]. All data were reduced to the latitude of Thessaloniki (40.65°N). The NRMS between the maximum likelihood curve and the data is 1.6, which indicates that a significant number of data could not be fitted and have been down-weighted by the I-RWLS algorithm. (d) Variations in Western Europe deduced from our data set and predicted at Paris by the regional archeomagnetic field model SCHA.DIF.3k [*Pavón-Carrasco et al*., 2009]. Both curves are reported with their errors at 95% confidence. (e) Variations in Western Europe computed at Paris from the global geomagnetic field models of *Korte et al*., [2009] (ARCH3k.1) and *Korte and Constable* [2011] (CALS3k.4).

the case for our data set (Figure 4a and Figure S3a, supporting information; see the contrast with Figures 4b and 4c and Figures S3b and S3c, supporting information). The self-consistency of the data set was also checked by computing the normalized residual root mean square (NRMS), which is the ratio between the *a posteriori* and the *a priori* intensity error of the data. In the present case, the NRMS is 1.1, thus close to 1 which indicates that the mean master curve fits the data within their *a priori* uncertainties. We stress that the bootstrap applied on the dating error always leads to smooth estimates of temporal magnetic field variations [see Figure 3 in *Thébault and Gallet* 2010]; for this reason, time variations in our master curve can be considered robust. The archeointensity master curve describes intensity variations that are characterized by a decreasing millennial timescale trend that is punctuated by three short intensity peaks, during the twelfth century, around the second half of the fourteenth century and at the transition between the sixteenth and the seventeenth centuries.

[16] If we exclude the new results presented here, a thorough comparison between the data obtained by *Genevey and Gallet* [2002] and *Genevey et al*. [2009] and other Western European archeointensity results dated to the past 800 years has already been discussed by *Genevey et al*. [2009]. We do not restate that comparison here. Since then, however, a new data set, which meets modern quality criteria, was obtained by *Schnepp et al*. [2009] from archeomagnetic analysis of an impressive succession of oven floors piled on top of each other during its long period of activity between ~1300 and ~1750 AD from a bakery in Lübeck, Germany. Although individually relatively poorly dated (with most age uncertainties >160 years), these results have regular intensity variations, which are similar both in shape and amplitude to the evolution shown in Figure 4a (Figure S2, supporting information). This independent data set, where data are strongly linked by a stratigraphic relationship, therefore supports the existence of rapid intensity variations since ~1200 AD.

[17] For the 900–1200 AD period, we used all available Western European data but selected only those fulfilling quality criteria. These criteria are exactly the same that those used for the past 800 years (and previously defined in *Genevey et al*. [2009]). They concern first the dating accuracy with an age uncertainty that must be less than 100 years (which, leads de facto to rejection of all but one older data point acquired by *Schnepp et al*. [2009]). Regarding the intensity protocol, the data must be acquired using the original or derived Thellier and Thellier method with partial TRM-check (pTRM-check) tests or with the original Shaw procedure. Furthermore, for objects generally recognized as strongly anisotropic, such as fragments of pottery or tiles, the TRM anisotropy effect must be taken into account. Finally, a minimum of three results is required per site (regardless of the definition of the site, i.e., fragment or

group of fragments) to retain a mean intensity value whose standard deviation should not exceed 15%. One result dated to the tenth century obtained by *Gómez-Paccard et al*. [2012] from architectural bricks collected from the famous Mont Saint-Michel church was retained, which appears to be in fairly good agreement with the observed decreasing intensity trend during the tenth century (Figure 4b). Six other data were also selected from *Gómez-Paccard et al*. [2006], which focused on a series of seven Spanish kilns archeologically dated to the twelfth century. These data are relatively scattered. This was first interpreted by *Gómez-Paccard et al*. [2006] as reflecting a limit in precision for intensity determinations. This dispersion, however, has the same order of amplitude as the intensity variations provided by our own data and, instead, could be linked to rapid intensity variations during the twelfth century. This is compatible with the fact that for three Spanish kilns there exists a stratigraphic relationship (with kiln "O" found under kiln "M", and the latter under kiln "L") and the corresponding mean intensity values progressively and systematically decrease in geomagnetic field intensity (Figure 4b). This possibility, not favored by *Gómez-Paccard et al*. [2006] (as another one they proposed in relation with the cooling rate effect) is now retained in *Gómez-Paccard et al*. [2012], in particular on the basis of an archeointensity data obtained from the Avranches castle, which however does not pass our selection criterion relying on the age uncertainties (>100 years).

[18] Altogether, there is a set of 86 selected (including our own) archeointensity data from Western Europe for the period spanning the past 11 centuries (Figure 4b). As in Figure 4a, probability density distributions were computed from this collection (see also Figure S3b, supporting information). For those computations, the chronological (relative) order available for the three previously mentioned Spanish kilns was taken into account by rejecting any curve estimate for which the bootstrapped data in question would not respect their temporal relationship. A similar case was also encountered for two other Spanish kilns dated to the fourteenth century [*Gómez-Paccard et al*., 2008]. The comparison between Figures 4a and 4b clearly indicates that incorporation of data with different origins and obtained by different experimenters significantly increases the data dispersion. As discussed by *Donadini et al*. [2009] and *Genevey et al*. [2008, 2009], this dispersion, which persists despite use of apparently stringent selection criteria, probably reflects relatively poor experimental determinations [e.g., *Fabian*, 2009; *Paterson et al*., 2012] and/or dating attribution for some data. The direct consequence is that, when data are averaged, their dispersion tends to smooth out rapid intensity variations seen in Figure 4a (i.e., the three peaks during the twelfth century, around 1350–1400 AD and ~1600 AD), although the overall signature remains unchanged (see also Figure S3, supporting information).

[19] We next compared Western European results with the large intensity data collection obtained from Eastern Europe, in Bulgaria [*Kovacheva et al*., 2009] and Greece, which was recently reexamined and updated by *Tema and Kondopoulou* [2011, see references herein]. Applying the same selection criteria as used for the Western European data, however, drastically reduces the number of intensity results from Eastern Europe, which makes it difficult to compare the two data sets (Figure 4c). To decipher this comparison, we tentatively released the constraint on the pTRM-checks for the Eastern European data (note that this modification, if it was applied, would not change the data collection previously discussed for Western Europe). This implies that the criteria on the number of individual values used to compute a mean and on the dispersion around the mean could indicate the absence of major magnetic alteration during intensity experiments for the retained data. The Eastern European data now selected appear relatively scattered but visually exhibit the same intensity variation pattern, with three intensity maxima, previously discussed for Western Europe (Figure 4c, see also Figure S3c, supporting information). This similarity therefore supports the fact that the intensity variations that are better observed in Western Europe over the past millennium may have occurred on a European scale [also see, *Gómez-Paccard et al*., 2012].

[20] We further compared our data set with values computed with the European archeomagnetic field model SCHA.DIF.3k [*Pavón-Carrasco et al*., 2009]. This model was developed for the period encompassing the past 3000 years using all available archeomagnetic directional and intensity data published before 2007. A loose selection was applied to exclude those data with age uncertainties longer than 500 years and with measurement uncertainties three times larger than the mean uncertainty computed from the whole collection. A weight was also associated to the data as a function of age and measurement uncertainties.

Regarding the intensity variation curve, the model mostly relies on the Eastern European data set (longitude >15°E), which represents more than 90% of the collection for 900–1850 AD. At Paris, this model predicts intensity variations whose pattern is similar to that displayed by our data set (Figure 4d). The three peaks appear, however, less well defined because of large error bars, and there is a time shift of ~75 years for the second peak which occurs earlier in the model (Figure 4d). Even if the intensity patterns are reasonably similar throughout Europe, as supported by this study [also see, *Gómez-Paccard et al*., 2012], the intensity data dispersion from Western and Eastern Europe currently limits both the resolution of the available regional geomagnetic model [*Pavón-Carrasco et al*., 2009] and the mean intensity variation curves that can be constructed at the subcontinental scale. This dispersion limits the use of intensity variations as an archeological dating tool.

[21] Scrutinizing the geographical extension of Western European intensity variations in other more distant regions is difficult because data that fulfill the quality criteria are neither numerous nor evenly distributed in time. This prevents recovery of detailed intensity variations, and, as a consequence, detection of possible rapid fluctuations outside of Europe [e.g., *Genevey et al*., 2008]. To tackle this question, another approach is to look at variations derived from global geomagnetic field models. We consider the ARCH3k.1 model [*Korte et al*., 2009] computed using only archeomagnetic data, whose reliability and resolution are considered higher in the northern hemisphere, and the recent CALS3k.4 model of *Korte and Constable* [2011], for which results from sedimentary records were also included (which probably induced recovery of smoother geomagnetic variations). Intensity variation curves derived at Paris from both models (Figure 4e) are unable to satisfactorily recover the rapid fluctuations mentioned above; these models therefore cannot help to define the geographical extension of those fluctuations. We note, however, that at longer multicentennial time scales, Western European data and the global field models agree concerning the general decreasing trend in geomagnetic field intensity over the past millennium (Figure 4e).

[22] The data reported in this study further allow re-examination of the question of the temporal coincidence in Western Eurasian regions between geomagnetic field fluctuations and climatic oscillations previously suggested by *Gallet et al*. [2005, 2006]. This hypothesis was initially based on the apparent correlation between geomagnetic intensity maxima detected in Western Europe during the past millennium and several colder periods documented by a succession of advances of the Swiss Grosser Aletsch glacier [*Holzhauser et al*., 2005]. It relied, however, on a limited intensity data set, with in particular a "missing" or "suspected" intensity peak during the twelfth century due to the lack of data for this time interval [*Gallet et al*., 2005, 2009b]. Since 2005, however, the Western European archeointensity database has been multiplied by more than a factor of four and a more thorough comparison can now be performed.

[23] We show in Figure 5a the climatic record provided by the Grosser Aletsch glacier together with the new well-defined archeointensity variation curve obtained for Western Europe. We used the Grosser Aletsch record, which is similar to that obtained from other glaciers in the Alps, because it provides a good synthesis of the main climatic fluctuations so far detected in Western-Central Europe during the past millennium. Its representativeness appears to be supported by data of different geological types with additional historical sources (Text S2, supporting information), which converge in defining several cooling periods during the twelfth and the fourteenth centuries, the second half of the sixteenth century and the first half of the nineteenth century. The three later events span the period referred to as the little ice age (LIA), which has been detected in glacier fluctuation records elsewhere in the world, as well as the cold period of the twelfth century [see, *Wanner et al*., 2008, and references therein]. We note that in the literature, the onset of the LIA can also be placed at the time of the cold episode at the end of the sixteenth century (e.g., discussion in *Matthews and Briffa* [2005, and references therein]). One can see from Figure 5a that the previous correlation observed by *Gallet et al*. [2005] still stands and appears reinforced by the more detailed data set, thanks in particular to the intensity peak during the twelfth century now better documented. Each of the three field intensity maxima detected during the past millennium is coincident, within age uncertainties, with a colder episode. However, the correlation between geomagnetic and climatic variations seems no longer valid after ~1700 AD (but see below). We quantified this observation and computed a distribution of correlation coefficients between the two detrended records between 900 AD and 1700 AD. This was carried out using a bootstrap procedure

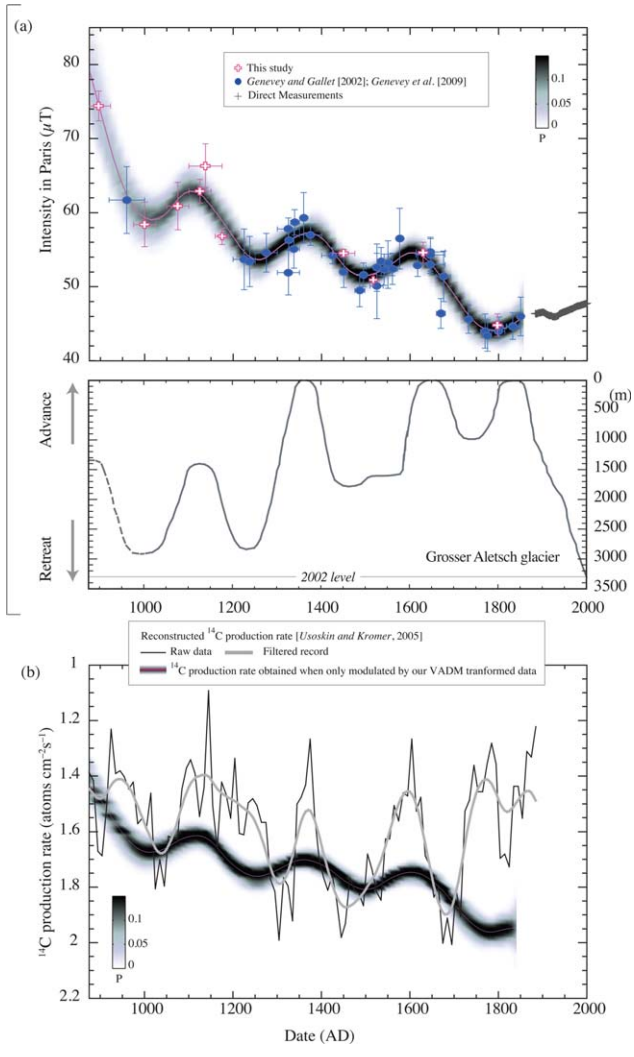

Figure 5. (a) Comparison of the Western European intensity variation curve deduced from our data set with fluctuations in the length of the Grosser Aletsch glacier [*Holzhauser et al*., 2005]. The dotted line indicates glacial advance that is currently less well documented. (b) Comparison between the ^{14}C production rate computed by *Usoskin and Kromer* [2005] (raw data and data filtered using a cutoff of ∼150 years) and the VADM-derived curve of ^{14}C production rates as deduced from our data set considering a constant solar magnetic activity (with a 500 MV modulation potential, *Kovaltsov et al*. [2012]). Note the inverted scale.

to generate a large ensemble of plausible intensity variation curves from the archeomagnetic data [*Thébault and Gallet*, 2010]. The histogram of coefficient correlations has a mean of ∼0.67 with a 95% confidence interval of 0.16 (Figure S4a, supporting information), thus confirming the good coherence observed between the two signals (Figure 5a). We acknowledge the fact that our intensity record is short and that a similar analysis on longer records is required to test further the possible geomagnetic-climatic connection. We could use archeointensity data for France and Spain [*Gómez-Paccard et al*., 2012] for the early High Middle Age (i.e., before 900 AD) for this purpose. However, this test would not be fully consistent because the data prior to and after 900 AD do not allow derivation of a master curve with a similar time resolution for all epochs. Nevertheless, *Gómez-Paccard et al*. [2012] proposed two intensity maxima during the High Middle Age, as previously suspected by *Gallet et al*. [2005] and *Gallet and Genevey* [2007] and also predicted by the European field model of *Pavón-Carrasco et al*. [2009], which again appear reasonably coincident in time with two successive advances of the Grosser Aletsch glacier [*Gallet et al*., 2005, 2009b].

[24] Together, the Western European archeointensity data seem to confirm a systematic temporal correlation over multidecadal timescales between

geomagnetic field intensity variations and climate [*Gallet et al*., 2009b]. The fact that it is apparently systematic argues for a causal relationship between the two phenomena. Although still a matter of strong debate, a possible mechanism for such a relationship could arise from a modulation of the galactic cosmic ray flux interacting with the atmosphere induced by large-scale changes in geomagnetic field geometry, perhaps associated with episodes of maximum hemispheric field eccentricity [*Gallet et al*., 2005, 2009a]. According to several authors (see for instance *Kirkby* [2007] for a discussion and references therein), this interaction may modify the production rate of clouds in the atmosphere, which would be an effective way of changing the climate.

[25] Having strengthened the hypothesis of a geomagnetic-climate connection, at least at the regional scale, we compared our Western European archeointensity data to changes in ^{14}C production rate reconstructed from the measured relative abundance of $\Delta^{14}C$ (IntCal04, *Reimer et al*. [2004]; *Usoskin and Kromer* [2005]). We first transformed the archeointensity results into virtual axial dipole moments (VADMs) and then computed the equivalent ^{14}C production rates assuming that they are only modulated by the VADM, i.e., considering a constant solar activity (Figure 5b). The error bars on this geomagnetic-derived ^{14}C variation curve were computed from the bootstrap procedure of *Thébault and Gallet* [2010]. Fourier analysis of the real ^{14}C and mean intensity time series shows rapid time variations for the former but no signal below ~150 years for the latter. We therefore filtered the "real" ^{14}C production rates using a cutoff of ~150 years, so that both the real and equivalent ^{14}C production rates share the same information content. These curves exhibit common patterns before 1700 AD, although there are noticeable differences between the amplitudes of variations between the two records (with smaller amplitudes for the geomagnetic-derived ^{14}C curve). The histogram of correlation coefficients shows a mean of $\sim 0.69 \pm 0.10$ (Figure S4b, supporting information), which quantitatively supports this visual impression. The mean decreases to $\sim 0.47 \pm 0.24$ when a long-term trend is subtracted from the two curves (Figure S4c, supporting information). Although moderate, this difference corroborates the fact that long-term ^{14}C production rate variations are principally controlled by changes in the geomagnetic field intensity averaged over several centuries, thus mainly reflecting the dipole field moment evolution [e.g., *Snowball and Muscheler* 2007]. It further illustrates the difficulty in ascertaining, but also in rejecting, a correlation at the century time scale between the real and geomagnetic-derived ^{14}C production rate variation curves using data spanning only the past millennium. It may be possible that at this time scale, the ^{14}C signal could result from combined geomagnetic and solar interactions, and that the geomagnetic contribution, having had its long-term trend subtracted, could be partly masked by the effects linked to solar activity fluctuations. We further note that the correlation here is complicated by possible non dipole field features in the geomagnetic-derived ^{14}C curve due to the regional nature of our archeointensity record. This complexity could explain the identification in Figure 5b of a common pattern of variation at certain periods, such as between the middle of the tenth and the beginning of the eighteenth centuries, which suggests a dipolar origin for the three observed intensity peaks. Available global field models are currently unable to recover these peaks (see Figure 4e). At other periods, a correlation appears more elusive. Much longer and more precise worldwide archeointensity records are needed to better constrain this issue. The approximate comparison over 0–1700 AD between the geomagnetic-derived ^{14}C curve computed from the geomagnetic field intensity model SCHA.DIF.3k [*Pavón-Carrasco et al*., 2009] at Paris and ^{14}C production rates (after filtering time variations shorter than ~150 years) gives a correlation coefficient of ~0.71 before and ~0.40 after detrending (Figures S4d and S4e, supporting information). These values are in agreement with the ones we obtained for a shorter time period. According to our hypothesis of a dual solar and geomagnetic origin for the centennial climate (Figure 5a) and radionuclide production variations (Figure 5b), the apparent loss of correlation after ~1700 AD might be explained by the overall decrease in geomagnetic dipole moment over the last 1000 years; the geomagnetic influence relative to solar forcing would have, hence, become less significant over the past three centuries.

5. Conclusions

[26] Our results support the existence of rapid European geomagnetic field intensity fluctuations over the past millennium, which are marked by the occurrence of three relative maxima. This work emphasizes the need to recover detailed century-scale geomagnetic field evolution at both regional and global scales not only for geomagnetic and archeological purposes but also to better decipher

the role of the geomagnetic field over multidecadal to centennial timescales in climate evolution either at regional or global scales and possibly for radionuclide production.

Acknowledgments

[27] The authors are grateful to the archeologists, historians, collection managers, and curators for their time and valuable help in collecting the archeological fragments: Clément Alix, Yvan Barat, Laurent Bourgeau, Caroline Kuhar Siffert, Marc Langlois, Françoise Lagarde, Annie Lefèvre, Claire Martin, Fabienne Ravoire, and Benoit Rouzeau. We are especially thankful to Jean Rosen with whom this work was initiated and who continues to actively help us in our search for well-dated fragments to analyze. This work was supported by the CNRS and the French Ministry of Culture. We are grateful to Vincent Courtillot for comments and to Ilya Usoskin for kindly providing us with ^{14}C production rate data. We thank A. Roberts, J. Pavón-Carrasco, M. Gómez-Paccard, and two anonymous reviews for helpful comments. We also thank Ruven Pillay for his valuable help on the manuscript. This is IPGP contribution n°3400.

References

Barat, Y., G. Debout, and M. Langlois (2010), Chevreuse, Donjon de la Madeleine (Yvelines, Île-de-France), Rapp. sondages, Service archéologique départemental des Yvelines, Montigny-le-Bretonneux, 37 pp.

Blanchard, P. (2010), Orléans, La Madeleine: Hospitalité et recueillement à travers différentes occupations (IXe—XVIIIe s.), Rapp. d'opération, Fouille archéologique, INRAP Cent.-Ile-de-France, France.

Casas, L., J. Shaw, M. Gich, and J. A. Share (2005), High-quality microwave archaeointensity determinations from an early 18th century AD English brick kiln, *Geophys. J. Int.*, *161*, 653–661.

Chauvin, A., Y. Garcia, P. Lanos, and F. Laubenheimer (2000), Paleointensity of the geomagnetic field recovered on archaeomagnetic sites from France, *Phys. Earth Planet. Inter.*, *120*, 111–136.

Coe, R. S. (1967), Paleo-intensities of the Earth's magnetic field determined from tertiary and quaternary rocks, *J. Geophys. Res.*, *72*, 3247–3262.

Courtillot, V., Y. Gallet, J.-L. Le Mouël, F. Fluteau, and A. Genevey (2007), Are there connections between the Earth's magnetic field and climate?, *Earth Planet. Sci. Lett.*, *253*, 328–339.

Donadini, F., M. Korte, and C. G. Constable (2009), Geomagnetic field for 0–3 ka: 1. New data sets for global modeling, *Geochem. Geophys. Geosyst.*, *10*, Q06007, doi:10.1029/2008GC002295.

Fabian, K. (2009), Thermochemical remanence acquisition in single-domain particle ensembles: A case for possible overestimation of the geomagnetic paleointensity, *Geochem. Geophys. Geosyst.*, *10*, Q06Z03, doi:10.1029/2009GC0024 20.

Gallet, Y., and A. Genevey (2007), The Mayans: Climate determinism or geomagnetic determinism ?, *EOS Trans. AGU*, *88*, 129–130.

Gallet, Y., and M. Le Goff (2006), High-temperature archeointensity measurements from Mesopotamia, *Earth Planet. Sci. Lett.*, *241*, 159–173.

Gallet, Y., A. Genevey, and V. Courtillot (2003), On the possible occurrence of archaeomagnetic jerks in the geomagnetic field over the past three millennia, *Earth Planet. Sci. Lett.*, *214*, 237–242.

Gallet, Y., A. Genevey, and F. Fluteau (2005), Does Earth's magnetic field secular variation control centennial climate change?, *Earth Planet. Sci. Lett.*, *236*, 339–347.

Gallet, Y., A. Genevey, M. Le Goff, F. Fluteau, and A. Eshraghi (2006), Possible impact of the Earth's magnetic field on the history of ancient civilizations, *Earth Planet. Sci. Lett.*, *246*, 17–26.

Gallet, Y., M. Le Goff, A. Genevey, J. Margueron, and P. Matthiae (2008), Geomagnetic field intensity behavior in the middle east between ∼3000 BC and ∼1500 BC, *Geophys. Res. Lett.*, *35*, L02307, doi:10.1029/ 2007GL031991.

Gallet, Y., G. Hulot, A. Chulliat, and A. Genevey (2009a), Geomagnetic field hemispheric asymmetry and archeomagnetic jerks, *Earth Planet. Sci. Lett.*, *284*, 179–186.

Gallet, Y., A. Genevey, M. Le Goff, N. Warmé, J. Gran-Aymerich, and A. Lefèvre (2009b), On the use of archeology in geomagnetism, and vice-versa: Recent developments in archeomagnetism, *C. R. Physique*, *10*, 630−648, doi:10.1016/j.crhy.2009.08.005.

Games, K. P., and M. E. Baker (1981), Determination of geomagnetic archaeomagnitudes from clay pipes, *Nature*, *289*, 478–479.

Genevey, A., and Y. Gallet (2002), Intensity of the geomagnetic field in western Europe over the past 2000 years: New data from ancient French pottery, *J. Geophys. Res.*, *107*(B11), 2285, doi:10.1029/2001JB000701.

Genevey, A., Y. Gallet, C. G. Constable, M. Korte, and G. Hulot (2008), ArcheoInt: An upgraded compilation of geomagnetic field intensity data for the past ten millennia and its application to the recovery of the past dipole moment, *Geochem. Geophys. Geosyst.*, *9*, Q04038, doi:10.1029/2007GC001881.

Genevey, A., Y. Gallet, J. Rosen, and M. Le Goff (2009), Evidence for rapid geomagnetic field intensity variations in Western Europe over the past 800 years from new French archeointensity data, *Earth Planet. Sci. Lett.*, *284*, 132–143.

Gómez-Paccard, M., A. Chauvin, P. Lanos, J. Thiriot, and P. Jiménez-Castillo (2006), Archeomagnetic study of seven contemporaneous kilns from Murcia (Spain), *Phys. Earth Planet. Inter.*, *157*, 16–32.

Gómez-Paccard, M., A. Chauvin, P. Lanos, and J. Thiriot (2008), New archeointensity data from Spain and the geomagnetic dipole moment in western Europe over the past 2000 years, *J. Geophys. Res.*, *113*, B09103, doi:10.1029/2008JB005582.

Gómez-Paccard, M., et al. (2012), Improving our knowledge of rapid geomagnetic field intensity changes observed in Europe between 200 and 1400 AD, *Earth Planet. Sci. Lett.*, *355–356*, 131–143.

Gram-Jensen, M., N. Abrahamsen, and A. Chauvin (2000), Archaeomagnetic intensity in Denmark, *Phys. Chem. Earth*, *25*, 525–531.

Hartmann, G. A., R .I. F. Trindade, A. Goguitchaichvili, C. Etchevarne, J. Morales, and M. C. Afonso (2008), First archeointensity results from Portuguese potteries (1550–1750 AD), *Earth Planets Space*, *61*, 93–100.

Hartmann, G. A., A. Genevey, Y. Gallet, R. I. F. Trindade, M. Le Goff, R. Najjar, C. Etchevarne, and M. C. Afonso (2011),

New historical archeointensity data from Brazil: Evidence for a large regional non-dipole field contribution over the past few centuries, *Earth Planet. Sci. Lett.*, *306*, 66–76.

Holzhauser, H., M. Magny, and H. J. Zumbühl (2005), Glacier and lake-level variations in west-central Europe over the last 3500 years, *Holocene*, *15*, 789–801.

Jesset, S. (2003), Chrono-typologie de la céramique d'Orléans et réseaux d'approvisionnement de la ville, in *La céramique médiévale et moderne du Centre-Ouest de la France (11e–17e siècle)*, edited by P. Husi, pp. 49–62, 20e supplément à la Revue Archéologique du Centre de la France, Tours.

Jesset, S. (2010), Les indices d'une manufacture de poterie de la fin du XVIIIe siècle à Orléans, *Rev. Archéologique du Loiret et de l'axe Ligérien*, *33*, 73–89.

Jesset, S. (2011), *Loiret, Fay-aux-Loges, Une poterie de la fin du Moyen Âge, Rapp. d'opération*, 278 pp., Fouille Archologique, INRAP Cent., France.

Kirkby, J. (2007), Cosmic rays and climate, *Surv. Geophys.*, *28*, 333–375, doi:10.1007/s10712-008-9030-6.

Korte, M., and C. G. Constable (2011), Improving geomagnetic field reconstructions for 0–3 ka, *Phys. Earth. Planet. Inter.*, *188*, 247–259.

Korte, M., F. Donadini, and C. G. Constable (2009), Geomagnetic field for 0–3 ka: 2. A new series of time-varying global models, *Geochem. Geophys. Geosyst.*, *10*, Q06008, doi:10.1029/2008GC002297.

Korte, M., C. Constable, F. Donadini, and R. Holme (2011), Reconstructing the Holocene geomagnetic field, *Earth Planet. Sci. Lett.*, *312*, 497–505.

Kovacheva, M., Y. Boyadziev, M. Kostadinova-Avramova, N. Jordanova, and F. Donadini (2009), Updated archeomagnetic data set of the past eight millenia from the Sofia laboratory, *Bulgaria, Geochem. Geophys. Geosyst.*, *10*, Q05002, doi:10.1029/2008GC002347.

Kovaltsov, G. A., A. Mishev, and I. G. Usoskin (2012), A new model of cosmogenic production of radiocarbon 14C in the atmosphere, *Earth Planet. Sci. Lett.*, *337*, 114–120.

Knudsen, M., and P. Riisager (2009), Is there a link between Earth's magnetic field and low-latitude precipitation?, *Geology*, *37*, 71–74.

Knudsen, M. F., P. Riisager, F. Donadini, I. Snowball, R. Muscheler, K. Korhonen, and L. J. Pesonen (2008), Variations in the geomagnetic dipole moment during the Holocene and the past 50 kyr, *Earth Planet. Sci. Lett.*, *272*, 319–329.

Lagarde, F., C. Brut, A. Lefèvre, and C. Martin (2011), Tour Saint-Jacques, Square de la Tour Saint-Jacques—Paris IVe, Rapp. de Fouille Archéologique d'urgence, 409 pp., Mairie de Paris.

Le Goff, M., and Y. Gallet (2004), A new three-axis vibrating sample magnetometer for continuous high-temperature magnetization measurements: Applications to paleo- and archeo-intensity determinations, *Earth Planet. Sci. Lett.*, *229*, 31–43.

Matthews, J. A., and K. R. Briffa (2005), The ''Little Ice Age'': Re-evaluation of an evolving concept, *Geogr. Ann.*, *87A*, 17–36.

McIntosh, G., M. Kovacheva, G. Catanzariti, F. Donadini, and M. L. O. Lopez (2011), High coercivity remanence in baked clay materials used in archeomagnetism, *Geochem. Geophys. Geosyst.*, *12*, Q02003, doi:10.1029/2010GC003310.

Paterson, G. A., A. J. Biggin, Y. Yamamoto, and Y. Pan (2012), Towards the robust selection of Thellier-type paleointensity data: The influence of experimental noise, *Geochem. Geophys. Geosyst.*, *13*, Q05Z43, doi:10.1029/2012GC004046.

Pavoń-Carrasco, F. J., M. L. Osete, J. M. Torta, and L. R. Gaya-Piqué (2009), A regional archeomagnetic model for Europe for the last 3000 years, SCHA.DIF.3K: Applications to archeomagnetic dating, *Geochem. Geophys. Geosyst.*, *10*, Q03013, doi:10.1029/2008GC002244.

Ravoire, F. (2007), *La céramique médiévale (fin du Xe-XVIe siècle)*, in Nevers, 12 rue Saint-Genest, fouilles de la partie méridionale de l'ancienne abbaye Notre-Dame et saint-Genest, chantier M.A.P.A.D., edited by B. Saint-Jean Vitus, Rapp. Final d'opération, Serv. Rég. de l'archéologie de Bourgogne, Inrap, Dijon.

Reimer, P. J. et al. (2004), IntCal04 terrestrial radiocarbon age calibration, 0–26 kyr BP, *Radiocarbon*, *46*, 1029–1058.

Roberts, A. P., Y. Cui, and K. L. Verosub (1995), Wasp-waisted hysteresis loops: Mineral magnetic characteristics and discrimination of components in mixed magnetic systems, *J. Geophys. Res.*, *100*, 17,909–17,924.

Rouzeau, B. (2009), Redécouvrir l'abbaye de Morimond à travers son site et ses bâtiments, paper presented at Culture et patrimoine cisterciens, 12 Jun, Collège des Bernardins, Paris, 31–43.

Rouzeau, B. (Ed.) (2010), *Ancienne abbaye de Morimond, Rapp. de fouille programmée*, 255 pp., Serv. Rég. d'Archologie Champagne-Ardennes, DFS, Châlons-sur-Marne.

Schnepp, E., P. Lanos, and A. Chauvin (2009), Geomagnetic paleointensity between 1300 and 1750 AD derived from a bread oven floor sequence in Lübeck, Germany, *Geochem. Geophys. Geosyst.*, *10*, Q08003, doi:10.1029/2009GC002470.

Snowball, I., and R. Muscheler (2007), Palaeomagnetic intensity data: An Achilles heel of solar activity reconstructions, *Holocene*, *17*, 851–859.

Suttie, N., R. Holme, M. J. Hill, and J. Shaw (2011), Consistent treatment of errors in archaeointensity implies rapid decay of the dipole prior to 1840, *Earth Planet. Sci. Lett.*, *304*, 13–21.

Tema, E., and D. Kondopoulou (2011), Secular variation of the Earth's magnetic field in the Balkan region during the last eight millennia based on archaeomagnetic data, *Geophys. J. Int.*, *186*, 603–614, doi:10.1111/j.1365-246X.2011.05088.x.

Thébault, E., and Y. Gallet (2010), A bootstrap algorithm for deriving the archeomagnetic field intensity variation curve in the middle east over the past 4 millennia BC, *Geophys. Res. Lett.*, *37*, L22303, doi:10.1029/2010GL044788.

Thellier, E., and O. Thellier (1959), Sur l'intensité du champ magnétique terrestre dans le passé historique et géologique, *Ann. Geophys.*, *15*, 285–376.

Usoskin, I. G., and B. Kromer (2005), Reconstruction of the 14C production rate from measured relative abundance, *Radiocarbon*, *47*, 31–37.

Usoskin, I. G., M. Korte, and G. A. Kovaltsov (2008), Role of centennial geomagnetic changes in local atmospheric ionization, *Geophys. Res. Lett.*, *35*, L05811, doi:10.1029/2007GL033040.

Usoskin, I. G., I. A. Mironova, M. Korte, and G. A. Kovaltsov (2010), Regional millennial trend in the cosmic ray induced ionization of the troposphere, *J. Atmos. Sol. Terr. Phys.*, *72*, 19–25.

Wanner, H., et al. (2008), Mid- to late Holocene climate change: An overview, *Quat. Sci. Rev.*, *27*, 1791–1828.